Egyptian Journal of Neurosurgery

RESEARCH Open Access

Traffic light alarming signs are indispensable prerequisites for fruitful endoscopic third ventriculostomy

Alhusain Nagm[1*]

Abstract

Background Endoscopic third ventriculostomy (ETV) is a satisfying neuro-endoscopic journey in candidates with preoperatively predicted higher success rates. Alarming cases require extra care to avoid serious complications, predict/identify failure and offer reasonable intra-/postoperative decisions.

Purpose To create easily interpretable traffic light alarming signs to increase the awareness level for neurosurgeons regarding ETV difficulty/failure.

Methods A 3-year-retrospective study of postoperative ETV infants of both sexes with obstructive hydrocephalus and preoperative ETV success score ≤ 70, age ≤ 12 months, and follow-up for ≥ 6 months with a postoperative radiological evaluation of the ETV patency and cerebrospinal fluid dynamics. The ETV difficulty scale (ETV-DS) was designed as an intraoperative monitor for surgical/anatomical difficulties. And the ETV failure threshold (ETV-FT) was offered for postoperative evaluation to identify cases that are mistakenly interpreted as failure.

Results Among our 159 case series, 54 infants were involved. Patients' demographics, age: ≤ 28 days, > 28 days to 6 months, and >6 to 12 months, were 5.5%, 70.3%, and 24.2%, respectively. Postoperatively, the outcome based on ETV-FT color scale was dark green (ETV-FT=0), light green (ETV-FT=1), yellow (ETV-FT=2), orange (ETV-FT=3), red (ETV-FT=4) in 29%, 14%, 20%, 10.3%, and 26.7%, respectively. Actual failure is identified as ETV-FT=4 based on clinical/radiological data. The failure rate was significantly attributed to inadequate communication with the basal cistern due to difficult/unsafe perforation of the thick/dense Liliequist membrane (87%) ($P = 0.001$).

Conclusion The traffic light alarming signs (ETV-DS and ETV-FT) can warn neurosurgeons to recognize critical cases that necessitate ultra-precautions to navigate safely through landmines for worthy outcomes.

Keywords Endoscopic third ventriculostomy, ETV failure, CSF flowmetry, Difficult, Traffic light

Introduction

In good candidates [1–3], and based on our triade [2] of proper candidate selection, surgical pearls to ensure rich communication between the third ventricle and basal cisterns, and appropriate postoperative management, endoscopic third ventriculostomy (ETV) will be an satisfying journey. The other side of the coin is the intraoperative unveiled events including, unique anatomical variables (>1/3 of cases) that increase the risk of intraoperative complications and associated with a 50% chance of early postoperative ETV failure [2–8]. Ensuring sufficient communication between the third ventricle (III-VT) and subarachnoid space and/or basal cisterns (SAS/BC) [2, 3], inevitability of additional procedures, cerebrospinal fluid (CSF) dynamics [2, 3, 9–18], and CSF pathway re-closure [19] can affect the outcome. Further,

*Correspondence:
Alhusain Nagm
nagm@azhar.edu.eg
[1] Department of Neurosurgery, Al-Azhar University Faculty of Medicine, 1 ElMokhayam El Daem St., Nasr City, Cairo 11884, Egypt

the well-known phenomenon of persistent/recurring increased intracranial pressure (↑ICP) in the initial postoperative adaptation period [20] is likely to be observed as a failure and misguidedly taken as a sign for shunt insertion [21–29]. Moreover, lack of preoperative tests predict the compliance and buffering capacity of the SAS/BC (which might account for an additional 25 to 40% failure rate) [30–33] and different thresholds for considering ETV failure [2, 3, 34–45] still limitations.

Herein, first, we designed a traffic light ETV difficulty scale (ETV-DS) as an intraoperative monitor to help neurosurgeons to be well prepared for challenging surgical/anatomical difficulties. Second, we proposed a postoperative traffic light ETV failure threshold (ETV-FT) that could be used to identify and manage cases that are mistakenly interpreted as failure.

Materials and methods

Study design, subject selection, duration, and intervention

The idea, design, administrative, technical, and material support by the corresponding author (AN). In compliance with ethical standards, the University's research ethics committee approval and consent, from all patients' parents/guardians who participated in this study, were obtained.

Availability of data and materials

The datasets used and/or analyzed during the current study are available from the corresponding author upon reasonable request.

This is a single-institution 3-year retrospective study done between July 2019 and September 2022.

Inclusion criteria

Inclusion criteria were as follows: postoperative ETV infants of both sexes with obstructive hydrocephalus due to aqueduct stenosis/tumor, post-hemorrhagic or post-infection with/without a history of previous shunt failure/complication, preoperative ETV success score [1] (ETV-SS) ≤ 70, age ≤12 months and follow-up for ≥ 6 months with postoperative phase-contrast magnetic resonance images (PC-MRI) cerebrospinal fluid (CSF) flowmetry to evaluate the ETV patency and ETV-CSF dynamics. All cases were operated with LOTTA® ventriculoscopes using the 4K-HD camera. Fogarty arterial embolectomy catheters (FAEC) (code 12A0805F/120805F) size 5F (inflated balloon diameter of 11 mm) were used to enlarge the ETV stoma. Tailored choroid plexus coagulation (CPC) was done only in selected infants with post-hemorrhagic hydrocephalus due to choroid plexus aneurysm-like structure (AnLS) to eliminate potential feeders (not as an augmenting procedure). ETV was an alternative when infants' parents/guardians refused shunt.

Exclusion criteria

Undoable ETV (inability to fenestrate the tuber cinerium), infants with other etiologies (including congenital anomalies) [44], active infection, compartmental (multicystic) hydrocephalus, age >12 months, received augmenting procedures (CPC)/postoperative lumber puncture, done with another ventriculoscopes/cameras/surgeon/institution, without postoperative CSF flowmetry, missed during the follow-up, refused ETV or unfit for surgery were excluded from this study.

The radiological protocol for postoperative evaluation of ETV patients was determined by two investigators, including an experienced independent radiologist, who was blinded to the patient's clinical data and the aim of the index study. Furthermore, the data of overall flow and stroke volumes across the stoma are measured by the machine's own software. Based on these two points, the influence of bias on research results can be excluded. Cine phase contrast (PC)-magnetic resonance image (MRI) CSF flowmetry was used for qualitative and quantitative assessment of ETV-CSF flow dynamics [6–12]. The traffic lights were assigned to the overall flow amplitude (OFA) [2, 6–12] to predict/interpret the response to surgery.

Statistical analysis

The collected data were tabulated, and SPSS 26.0 was employed for statistical analysis along with Microsoft Excel 2016 and MedCalC program software version 19.1. A value of $P < 0.05$ was considered significant.

Traffic light alarming signs (ETV-DS and ETV-FT) (Figs. 1, 2)

ETV-DS (Fig. 1) focused on six parameters

1. Third ventricular (III-VT) anomaly that hinders the freedom for ETV stoma maneuverability (such as hypothalamic adhesions (Fig. 3)), ventricular wall deposits, presence of AnLS (Figs. 3, 4, 5).
2. Tuber cinerium (TC) types (Fig. 3).
3. stoma size
4. Liliequist membrane (LM) types/leaflets (Figs. 3, 4, 5, 6).
5. Visual confirmation of specific neurovascular structures in SAS/BC (naked basilar artery (BA)/presence of dolicoectatic BA (DEBA) (Fig. 6)/ brainstem and cranial nerve identification) (Figs. 3,4, 5, 6).
6. CSF appearance (Fig. 5).

	0	1	2
III-VT anomaly that hinders the freedom for ETV stoma maneuverability/ VT wall deposits (§)	No	Relevant anatomical variations (ENFM, mFM, AnLS, significant thalamic/hypothalamic adhesions, crowded III-VT floor) **(*)** +/- VT wall deposits. *or* Tumors filling III-VT = failure to reach the floor *(following debulking, CSF flow via Aq.Slv is feasible)* **(#)**	Phantom III-VT *"No Man's Land SAS/BC"* (= all pertinent agreed landmarks are absent: scout around for DS) *or* Tumors filling III-VT = failure to reach the floor *(neither ETV nor CSF flow via Aq.Slv)*
Tuber cinerium	Thin/ translucent	Thick/ opaque *or* congested	–
Stoma size	≥10mm **(¶)**	6-9mm	≤5mm
LM-DL	Fenestrated	Thin membranous	Thick dense/scar engulfing the perforators
Naked basilar artery (LM-ML) / DEBA / Identified CN (ǂ)	Whole artery without DEBA/ identified CN	–	Covered bifurcation and/or trunk +/- unidentifiable CN *or* DEBA
CSF (‡)	Clear	Turbid/ colored	–

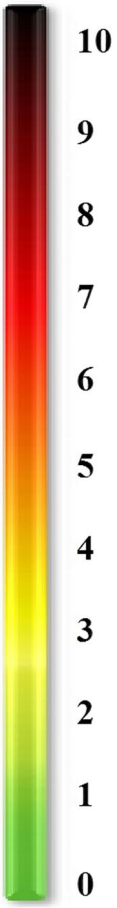

Fig. 1 ETV difficulty scale. Serious intraoperative findings that haunts neurosurgeons and can be encountered during ETV journey and could predict achievability/difficulty. Difficultly is directly proportional to the ETV-DS (the higher the score, the higher the alarming sign = tendency to face a challenging operation/ complications, require special surgical pearls and predict ETV failure): (ETV) endoscopic third ventriculostomy, (III-VT) third ventricle, (§) including post-hemorrhagic deposits and/or postinfectious debris, (ENFM) extreme narrow foramen of Monro, (mFM) membrane masking the foramen of Monro, (AnLS) aneurysm-like structure, (*) achievable: can be opened surgically, (Aq.Slv) aqueduct of Sylvius, (#) ETV seems impossible "in our hands" as we could not reach the III-VT floor, therefore, we ensure reasonable CSF flow via debulking of the posterior part of the tumor that covers the Aq.Slv., (SAS/BC) subarachnoid space/ basal cisterns, (DS) dorsum sellae, (¶) measured with the maximal diameter of Fogarty arterial embolectomy catheters (FAEC) (code 12A0805F/120805F) size 5F (inflated balloon diameter of 11 mm), (LM-DL) Liliequist membrane diencephalic layer, (DEBA) dolicoectatic basilar artery, (LM-ML) Liliequist membrane mesencephalic layer, (CN) cranial nerve, (ǂ) oculomotor (III) and/or abducent (VI) nerves in the basal cisterns, (CSF) cerebrospinal fluid, (‡) initial sampling before irrigation/lavage and at the end of the procedure if iatrogenic hemorrhagic insult occurred

ETV-FT (Fig. 2)

It is proposed to overcome the different thresholds for considering ETV failure [1, 20–22]. ETV-FT focused on two parameters: I) evaluation of ETV stoma with CSF flowmetry and II) clinical picture.

Surgical technique and illustrative cases

Surgical nuances

Our step-by-step technique can be reviewed elsewhere [2]. We always consider the "curved reservoir skin incision with subgaleal pocket technique" in all cases [2, 4].

III-VT floor Tumor biopsy/resection

We ensure reasonable CSF flow by debulking of the posterior part of the tumor that covers the Aq.Slv.

Dealing with phantom III ventricle (Figs. 6, 7) "NO Man's Land SAS/BC"

In infants with post-infection hydrocephalus, the regular anatomy is unclear and the landmarks are totally lost (we defined it as phantom III ventricle). Besides, the SAS/BC for these infants were considered as "No Man's Land" (undoable ETV). We always scout around for clivus/dorsum sellae (DS) as the only reliable buried turning point.

	0	1	2	
Evaluation of ETV stoma with Cine PC-MRI CSF-flowmetry (¶) 2 weeks postoperatively: qualitatively and quantitatively	Grade III (patent stoma with adequate flow; OFA value ≥75 µL)	Grade II (patent stoma with low flow; OFA value from 25 up to <75 µL) **(§)**	Grade I (obstructed stoma/ patent stoma with impaired flow; OFA value <25 µL) **(§)**	**4**
Clinical picture: including ↑ICP, SG-CSF collection +/- CSF leak	Complete improvement = resolution of all symptoms and signs of ↑ICP *without* SG-CSF collection or CSF leak	Gradual improvement= insistent/ early recurring ↑ICP within the initial adaptation-period that is rapidly normalized with single/repeated LP **(#)** *and/or* Type I SG-CSF collection **(‡)** +/- controllable low-flow/clear CSF leak	True/impending failure= Persistent/ late recurring ↑ICP within 6 months that is resistant to LP *or* due to stoma reclosure after 6 months (*) *and/or* Type II SG-CSF collection (ǂ) +/- uncontrollable high-flow and/or colored CSF leak	**3** **2** **1** **0**

Fig. 2 ETV failure threshold. Threshold to identify ETV failure during early postoperative follow-up = Failure is directly proportional to the ETV-FT (the higher the score, the higher the tendency to show ETV failure): The failure threshold is defined as two red signs or score "4." (ETV) endoscopic third ventriculostomy, (¶) cine phase contrast (PC)-magnetic resonance image (MRI) cerebrospinal fluid (CSF) flowmetry for qualitative and quantitative assessment of CSF flow dynamics through the ETV stoma to assess its patency: Qualitatively by observing the pulsatile CSF flow at mid-sagittal image. Quantitatively by measuring the region of interest (ROI) at ETV stoma on 3D steady state free precession (SSFP) images sequence with thin cuts that allows flow quantification and better CSF assessment, (OFA) overall flow amplitude: the most effective variable to predict the response to surgery. NB: Early postoperative flow index (FI) >40% is significantly linked with successful ETV. FI= (stroke volume of prepontine cistern / stroke volume of interpeduncular cistern) ×100, (§) patent stoma with low/impaired flow might be due to the presence of another CSF diversion pathway (internal drainage due to reopening of the aqueduct again after removal of tumor or cyst), (↑ICP) high intracranial pressure, (SG) subgaleal, (CSF) cerebrospinal fluid, (POD) postoperative day, (LP) lumbar puncture , (#) during the initial adaptation-period on POD-3/5 or within 2 weeks after ETV, (SAS) subarachnoid space, (ǂ) Type I SG-CSF collection: transient/ soft without CSF leak (or CSF leak from the SAS) during the adaptation-period, (‡) Type II SG-CSF collection: permanent/ tense without CSF leak (or controllable low-flow/clear CSF leak) during the adaptation-period, (*) stoma closure with new arachnoid membrane/scar. Uncontrollable high-flow and/or colored CSF leak

(See figure on next page.)

Fig. 3 Neuroendoscopic video-captured images from 10 different cases showing the inter-(hypo)thalamic adhesions (**A**, **B**), types of tuber cinerium (TC) (**C**–**E**), types of Liliequist membrane (LM) and beautiful visual confirmation (F-H): **A**, **B** 2 different cases showing that the hypothalamic adhesions are III-VT anomaly that hinders the freedom for ETV stoma maneuverability. (**A**) Massa intermedia (MI) to be differentiated from (**B**) Hypothalamic adhesions (hypoth adhesions). *TC: tuber cinerium, MB: mammillary bodies, CP: choroid plexus, PC: posterior commissure, star aqueducst os Sylvius.* (**C**–**E**) types of tuber cinerium (TC) in 6 different infants, **C** thin transparent TC in 4 different infants (large and upper/middle/lower insets) where the deeper structures (including basilar artery (BA), dorsum sellae (DS)) can be seen. Besides, the infundibular recess (inf) and mammillary bodies can be evaluated. Upper, middle and lower insets showing other examples of thin transparent TC with different degrees of visualization of deeper structures. **D** Congested type with engorged veins hindering the ETV (ǂ) (= yellow sign) and how to overcome this (insets). **E** Thick opaque type with III-VT wall deposits/pigmentations (#). **F**–**H** 2 different cases showing the importance to open the LM and visual confirmation of the basal cistern (= green sign). **F** The structure within the SAS/BC can be seen behind the thin LM "including basilar artery (BA), dorsum sellae (DS)." Besides, the oculomotor nerve (III) and uncus of temporal lobe (TL) can be seen via the created stoma. **G** Following reasonable opening of the LM, the pituitary fossa (PF), DS, posterior clinoid process (PCP), naked BA, brainstem (BS), III, TL, anterior petroclinoid ligament (¶) and porus occulomotaris (§) are confirmed. **H** Another example: after realistic distal opening of LM we can appreciate the foramen magnum (FM), right abducent nerve (VI) entering the Drello's canal (DC) (= green sign). BA with its perforators to the brainstem, right oculomotor (III) are confirmed

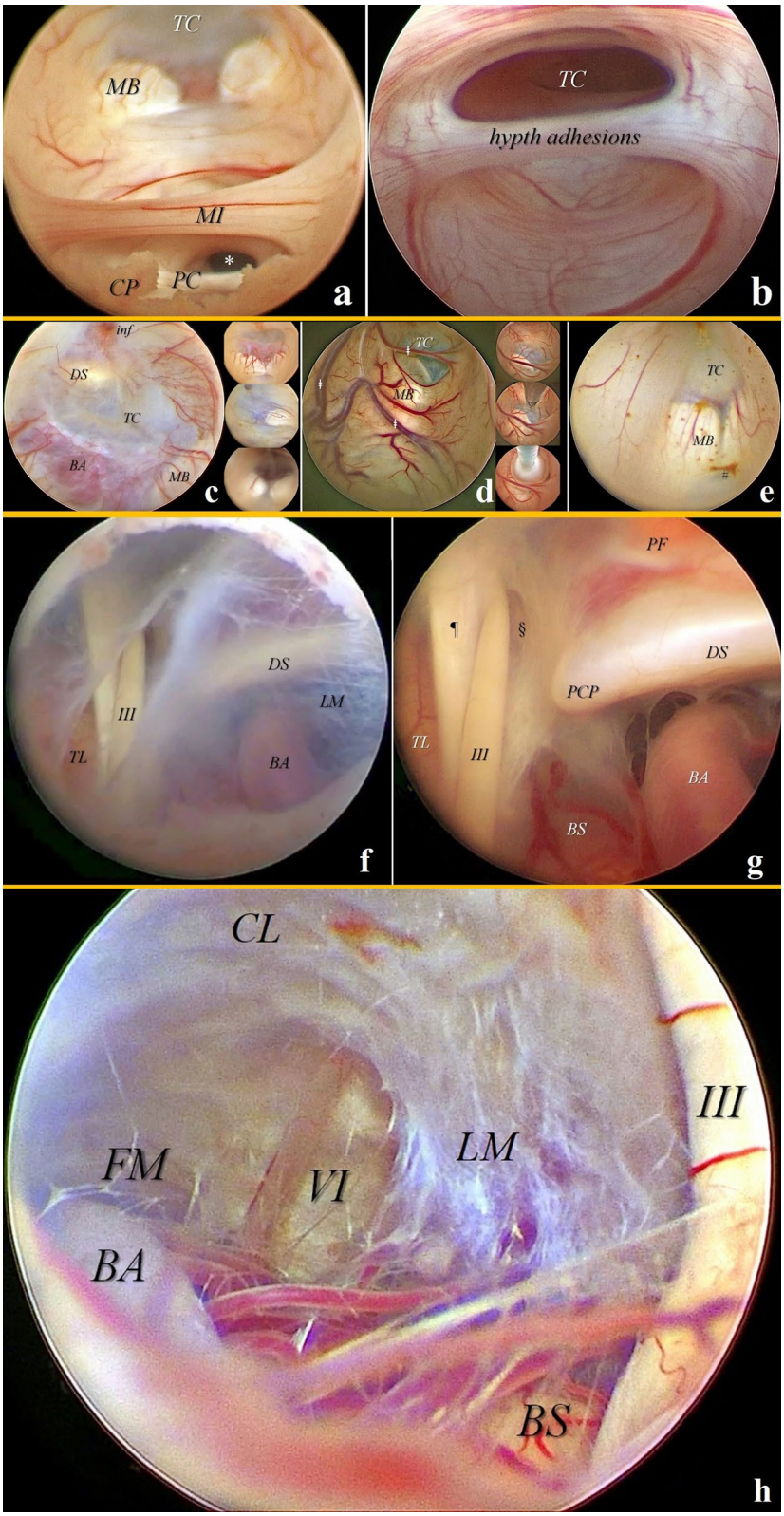

Fig. 3 (See legend on previous page.)

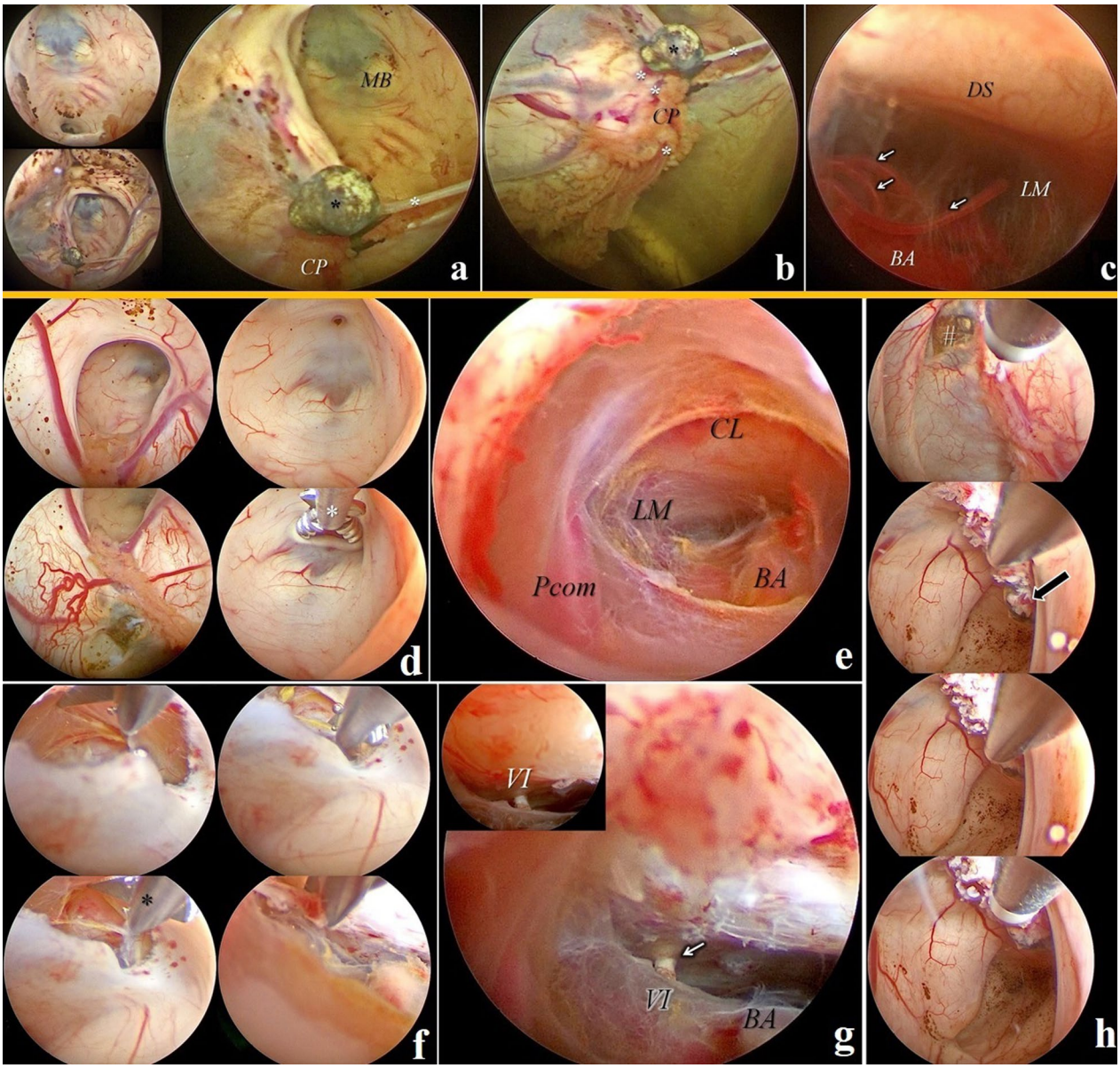

Fig. 4 Neuroendoscopic video-captured images showing aneurysm like structure (AnLS) in 2 different neonates: (**A**–**C**) in a 3-day-old male neonate. **A** Evidence of post-hemorrhagic brown pigmentations are seen along the lateral/third ventricular walls (lower inset) and inside the aqueduct of sylvius (upper inset). The III-VT structures (including mamillary bodies "MB") are seen before navigating the foramen of Monro. The AnLS (black star) can be seen along the choroidal vessels and vessels around the foramen of Monro (white stars) = yellow sign. **B** Showing the relationship between the choroid plexus (CP), AnLS (black star) and related vessels (white stars). **C** visual confirmation of the basal cistern showing the dorsum sellae (DS), basilar atery (BA) and its perforators and major branches (white arrows) surrounded by our openings in the thin/transparent Liliequist membrane (LM). (**D**–**H**) in a 28-day-old male neonate. **D** Evidence of post-hemorrhagic brown pigmentations (= yellow sign) are seen along the lateral ventricular walls and choroid plexus and Decq forceps (white*) opened parallel to the clivus to do an ETV stoma (lowr right inset). The III-VT structures are seen before navigating the foramen of Monro. **E**, **F**, **G** visual confirmation of the basal cistern showing the clivus (CL), basilar artery (BA), Posterior communicating artery (Pcom) and a thick dense Liliequist membrane (LM) (= red sign). **F** Stepwise opening the thick/dense LM with scissors (black*). **G** The abducent nerve (VI) was finally identified entering the Drello's canal (white arrow). **H** At the end CPC was added to both agument the ETV and, to elimenate the AnLS feeders which was seen along the choroid plexus inside the temporal horn (black arrow)

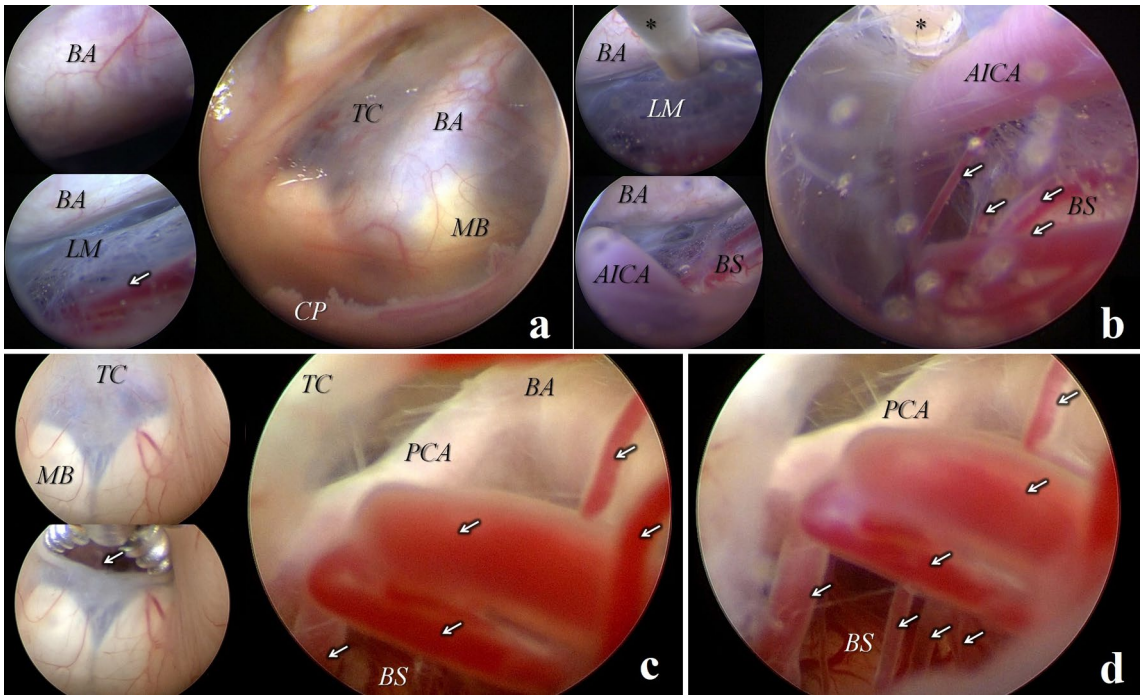

Fig. 5 Neuroendoscopic video-captured images showing challeging ETV in two different cases with dolicoectatic basilar artery (DEBA). **A** A view via the left foramen of monro "choroid plexus (CP)." The basilar artery (BA) is seen indenting the tuber cinerium (TC), pushing it upwards and separating the mammillary bodies (MB). The upper inset showing the naked BA after ETV. The lower inset showing a thick/dense Liliequist membrane (LM) covering the perforators (white arrow) and brainstem. It has to be opened to ensure adequate CSF communication with the SAS/BC. **B** Upper inset showing opening LM around the DEBA with Fogarty catheter (*). Following LM fenestration, the anterior inferior cerebellar artery (AICA), brainstem (BS) and perforators are confirmed (white arrows). **C**, **D** Another case showing the basilar bifurcation (BA), posterior cerebral artery (PCA) and perforators immediately after TC opening (white arrows). The brainstem (BS) and perforators are naked and obviously seen. Notice the fenestrated LM

In those cases the DS as a bony structure can be traced and palpated.

Results

Patients' demographics (Table 1)

Among our 159 case series, 54 patients were included in this study. Our included candidates showed slight male predominance (61.4%). Age ≤ 28 days (neonates), > 28 days to 6 months (babies), and >6 to 12 months (young infants) were 5.5%, 70.3%, and 24.2%, respectively. Obstructive hydrocephalus due to aqueductal stenosis, aqueductal tumor, post-hemorrhagic, post-infection or others was 81.6%, 5.5%, 3.7%, 3.7%, and 5.5%, respectively. All neonates were presented with post-hemorrhagic hydrocephalus, whereas aqueductal stenosis was common among babies young infants. ETV with the opening of LM and visual confirmation of the basal cisterns were achieved in all cases. Tumor biopsy was done in all tumor cases (5.5%). The histopathology of biopsied cases revealed, subependymoma or astrocytoma, in 66.6% and 33.4%, respectively.

Pertinent anatomy

In the index study, we realized three types of TC (Fig. 3) thin/transparent (green sign), congested (green sign) and thick/opaque (yellow sign) in 57%, 4% and 39%, respectively. Besides, three types of LM (Fig. 3,4,5,6) were observed: thick/dense (33.3%), thin/transparent (63%), and fenestrated (3.7%). The failure rate was significantly attributed to inadequate communication with the basal cistern due to difficult/unsafe perforation of the thick/dense LM (87%) (P = 0.001), particularly in infants ≤6 months, stoma closure with scar formation (3.7%), delayed post-meningetic sequences (5.6%) or other (3.7%).

ETV-DS and ETV-FT

Intraoperatively, the traffic light ETV-DS with its color scale was green (ETV-DS= ≤1), Yellow (ETV-DS=2-4), orange/red (ETV-DS=5-8), and black (ETV-DS=≥9), in 3.7%, 59.3%, 33.3%, and 3.7%, respectively.

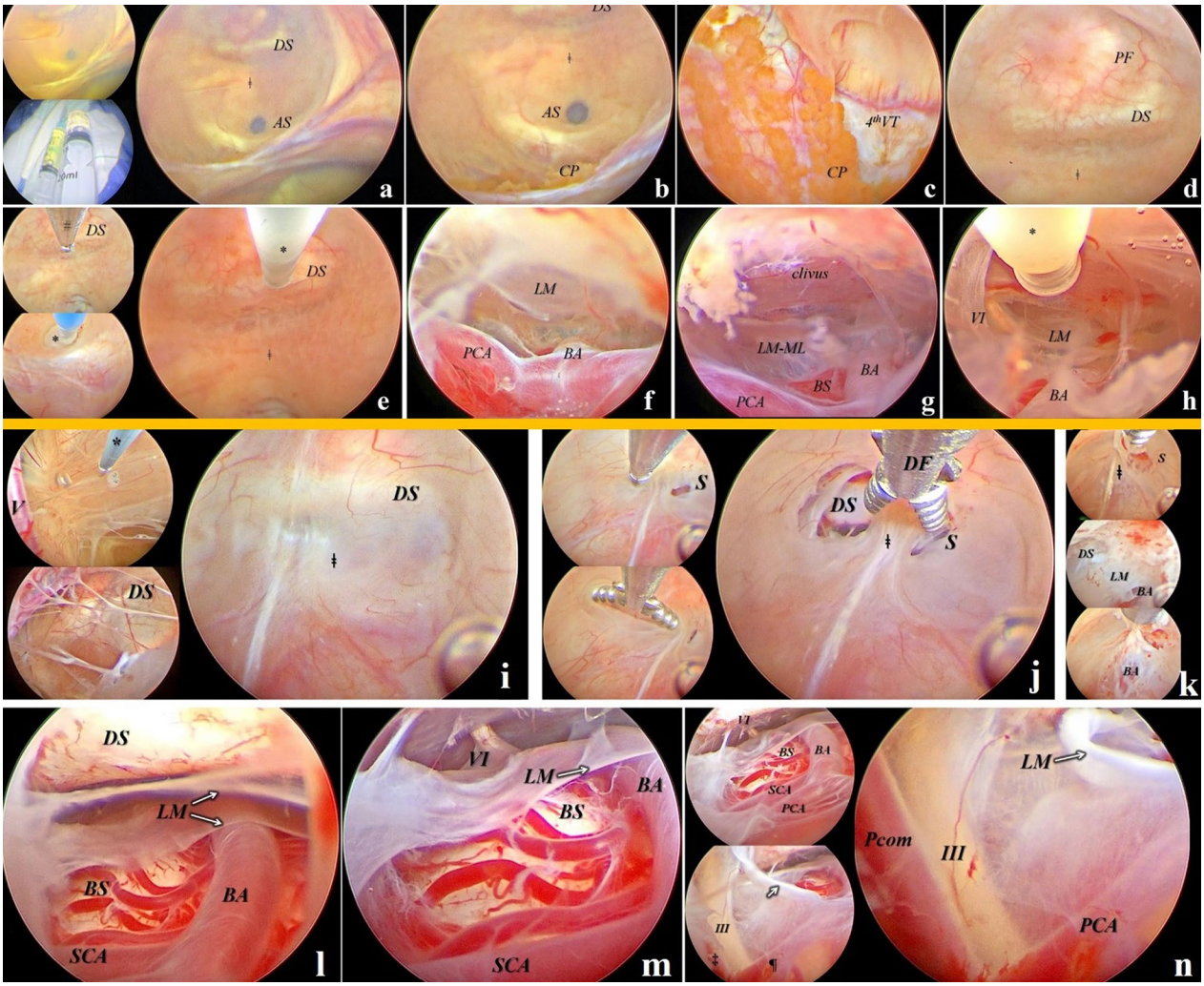

Fig. 6 Neuroendoscopic video-captured images showing phantom III-VT in 2 different babies (= black sign). (**A**-**H**) first baby: **A**, **B** Yellowish CSF can be seen. Lower inset comparing the initial syringe containing yellow CSF "left" and final clear result "right" after endoscopic lavage and replacement with CSF substitute. No landmarks at all. Scout around for the dorsum sellae (DS) to imagine the III-VT floor (ǂ) between the DS and aqueduct of Sylvius (AS). Notice the choroid plexus (CP) of the everted III-VT roof. **C** A view through the AS showing the yellowish discoloration of the CP of the fourth ventricle (4th VT). **D** Close view to the site of expected ETV stoma: Pituitary fossa (PF), DS, floor (ǂ). **E** Palpation of the DS with Fogarty catheter (*), perforation with Decq forceps (#: upper inset) and enlarging the stoma with balloon (*: lower inset). **F** Naked basilar artery (BA) and exposed posterior cerebral artery (PCA) are not enough as the thick/dense Liliequist membrane mesencephalic layer (LM-ML) still preventing adequate CSF communication with SAS/BC (= red sign). **G**, **H**) following several attempts to open the LM-ML, the clivus (CL), brainstem (BS) and left abducent nerve (VI) are exposed. However, it was extremely difficult and hazardous. **I–N** showing another baby with phantom III-VT (= black sign). **I** Cutting the intraventricular synechiae beside veins (V) with bipolar electro-cautery (*) to face a phantom III-VT floor (ǂ) and scout around to find the DS. **J** stepwise stoma creation just behind the DS with Decq forceps (DF) which is used to create 2 stomas with closed DF (upper inset) then open it parallel to the clivus (lower inset) and try to put each blade of DF inside each stoma to start dissection. **K** Thick multilayered LM is seen beyond the phantom III-VT floor and initial exposure of the basilar artery (BA). **L** BA, superior cerebellar artery (SCA), brainstem (BS), DS and multilayered thin/transparent LM (white arrows) are seen. **M** removing on layer of LM exposing the left abducent nerve (VI). **N** lateral view showing the left oculomotor nerve (III) in the angle between the posterior cerebral artery (PCA/¶) and posterior communicating artery (Pcom/ǂ) and its relation to the created stoma within the thin/transparent LM (white arrow). Upper and lower insets demonstrating different magnifications to catch a panoramic view

Postoperatively, the traffic light ETV-FT was green, yellow, and red in 43%, 20%, and 37%, respectively, while the ETV outcome based on ETV-FT color scale (Fig. 7) was dark green (ETV-FT=0), light green (ETV-FT=1), yellow (ETV-FT=2), orange (ETV-FT=3), red (ETV-FT=4) in 29%, 14%, 20%, 10.3% and 26.7%, respectively. Favorable outcome was documented in 63% (dark green, light green, and yellow), while

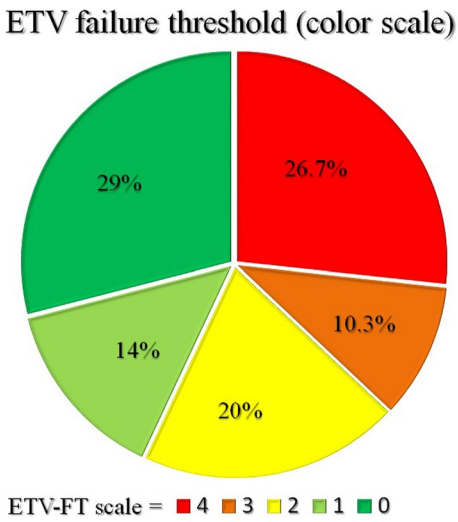

Fig. 7 ETV outcome based on ETV-FT color scale. Showing the percentage of true failure (ETV= 4 "red"), impending failure (ETV= 3 "orange") that requires close follow-up, favorable outcome (ETV= 2 "yellow," ETV= 1 "light green," and ETV= 0 "dark green")

unfavorable outcome was unveiled in 37% (orange and red) (Table 1).

Interpretation of ETV-DS (Fig. 1) and ETV-FT (Fig. 2)

ETV-DS (traffic light and scoring system): Difficultly is directly proportional to the ETV-DS and color grading scale. The green, yellow, and red traffic lights are assigned for straightforward communication with SAS/BC, difficult-but-achievable, and complex cases that require advanced skills, respectively. Black color is assigned for the most ever challenging anatomy that we called "phantom III-VT."

ETV-FT (traffic light and scoring system)

The failure threshold is defined as two red signs = score "4." Failure is directly proportional to the ETV-FT score and color grading scale. The green, yellow, and red traffic lights are assigned for patent stoma with adequate flow & complete resolution of symptoms, patent stoma with gradual resolution of symptoms during the adaptation-period [20–27] and obstructed stoma with failure, respectively.

We defined ETV success as the resolution of symptoms with a patent stoma on the postoperative CSF flowmetry and uneventful 6-month follow-up. While ETV true failure was defined as persistent symptoms (including progressive head enlargement) that are resistant to postoperative CSF release (adaptation failure) with an obstructed stoma on the postoperative CSF flowmetry during 6-month follow-up. Our actual failed ETV cases received another intervention (redo-ETV or shunt) for CSF diversion.

Complications (Table 1)

Entirely intraoperative negatives were referred to unintentional damages around the FM including unilateral minor injury "red spots" to the column of the fornix (2%) which was attributed to the torque effect of the rigid endoscope around the FM during tumor biopsy or ETV via an extremely narrow FM [2, 4]. Controllable bleeding due to minor injury to venous structures (3.7%). Besides, we had a baby with intraoperative subdural hematoma (0.5%) following the dry filed technique for hemostasis that mandated immediate endoscopic evacuation. Additionally, another baby developed significant postoperative subdural hygroma (0.5%) and required subdural-peritoneal shunt to resolve his symptoms. Those cases had an uneventful postoperative course.

Neither tension pneumocephalus nor serious major neurovascular injuries (intact vertebrobasilar arteries, perforators, major veins, cranial nerves, brainstem, mammillary bodies, optic apparatus, infundibulum, (hypo) thalamus and basal ganglia).

Subgaleal (SG)-CSF collection/leak (Table 1)

Tense SG collection (type II/red sign) was seen in 7.4% of cases, mostly in age ≤6 months. Among them, 5.6% showed at least on attack of CSF leak during the early adaptation-period which was controlled with conservative measures. Two of CSF leak babies developed post-meningitic sequelae (3.7%) with delayed ETV failure and required another intervention. Yet, soft SG collections (type I/yellow sign) in 22% were resolved spontaneously. In those cases (except 3.7% post-meningitic sequelae), follow-up CSF flowmetry revealed good flow across the stoma.

Discussion

Anatomy, surgical nuances, and concerns to be valued while producing the ETV-DS

Interestingly, ventricular wall inspection for deposits and CSF nature can give additional vital information. In neonates, post-hemorrhagic ventricular wall pigmentations were linked to ruptured AnLS (Fig. 3,4) in 3.7%, and post-infection debris was linked to phantom III-VT in 3.7% (Fig. 7,8). We realized that ventricular wall deposits are often associated with difficult communication between the III-VT and SAS/BC due to thick dense LM in 33.3%. Moreover, congested and thick/opaque types of TC [24, 26, 43] can influence the stoma creation in 43% which became more challenging in the presence of inter-(hypo) thalamic adhesions.

Table 1 Patients' demographics: (*) significant

Case series	Total number			159
	Excluded			105
	Included			54
Age (*infants*)	≤ 28 days *(neonates)*			5.5%
	> 28 days to 6 months *(babies)*			70.3%
	>6 to 12 months *(young infants)*			24.2%
Sex	Male			61.4%
	Female			39.6%
Etiology	Aqueductal stenosis			81.6%
	Aqueductal tumor			5.5%
	Post-hemorrhagic			3.7%
	Post-infection			3.7%
	Others			5.5%
Histopathology	Subependymoma			66.6%
	Astrocytoma			33.4%
Types of TC	Thin/transparent			57%
	Congested			4%
	Thick/opaque			39%
Types of LM	Thick/dense			33.3%
	Thin/transparent			63%
	Fenestrated			3.7%
ETV-DS	Green *(straightforward communication with SAS/BC)* (ETV-DS= ≤1)			3.7%
	Yellow *(difficult-but-achievable ETV)* (ETV-DS=2-4)			59.3%
	Orange and Red *(complex cases that require advanced skills)*(ETV-DS=5-8)			33.3%
	Black *(including phantom third ventricle)*(ETV-DS=≥9)			3.7%
ETV-FT	Green *(adequate flow & complete resolution of symptoms)*			43%
	Yellow *(patent stoma with gradual resolution of symptoms during the adaptation-period)*			20%
	Red *(obstructed stoma with persistent symptoms "including progressive head enlargement" that are resistant to postoperative CSF release)*			37%
Outcome = ETV-FT color scale	Dark green (ETV-FT=0)	29%	Favorable	63%
	Light green (ETV-FT=1)	14%		
	Yellow (ETV-FT=2)	20%		
	Orange (ETV-FT=3)	Impending failure (10.3%)	Unfavorable	37%
	Red (ETV-FT=4)	Actual failure (26.7%)		
Failure (impending/ true)-related factors	Difficult/unsafe perforation of the thick/dense LM (*P = 0.001*)*			87%
	Stoma closure with scar formation			3.7%
	Delayed post-meningetic sequences			5.6%
	Other			3.7%
Complications	Unilateral minor injury "red spots" to the column of the fornix			2%
	Controllable bleeding due to minor venous injury around FM			3.7%
	Ipsilateral postoperative subdural hygroma (subdural-peritoneal shunt)			0.5%
	Intraoperative acute subdural hematoma (immediate endoscopic evacuation)			0.5%
	Postoperative CSF leak			5.6%
	Post-meningitic sequelae			3.7%
	Tension pneumocephalus			-
	Serious major neurovascular injuries			-
Subgaleal-CSF collection	Soft (type I) without CSF leak			22%
	Tense (type II) +/- CSF leak			7.4%

Radiological facts that we consider while designing ETV-FT

1- PC-MRI CSF flowmetry is considered more accurate/reliable for evaluating the patency of ETV [7, 8] and assessing ETV-CSF dynamics [6–12].
2- Ventricular size reduction is often slow with minimal/no changes [13].
3- The BA pulsation produces a flow void in the prepontine cistern that may interfere with the interpretation flow void that seen on T2-MRI at ETV stoma. Therefore, the absence of this void does not necessarily indicate impaired ETV function [6–12].
4- Early postoperative turbulent flow at the ETV stoma in the first CSF-flowmetry does not inevitably postulate failure. Such finding progressively returns to normal [15].
5- Greater stroke volumes (adequate flow=Grade III) [26] at the ETV stoma are a positive judge of favorable clinical outcome. Consequently, in patients with low/impaired flow (Grade II/I) [26] it might predict unfavorable clinical outcomes and further careful observation is vital as they may progress to occlusion [16].
6- If a patent ETV stoma is detected without sufficient CSF flow, this might be attributed to the existence of an alternative CSF diversion pathway (ex: internal drainage due to reopening of the aqueduct following removal of tumor) [17, 18].

Postoperative clinical facts during the adaptation-period

CSF dynamics/absorption, ICP, and rule of curved reservoir skin incision with subgaleal pocket technique:

1. The ICP does not decrease quickly in definite cases as it takes several months for CSF absorptive capacity/dynamics through the SAS/BC to show further improvement [22].
2. During the ETV initial postoperative adaptation period, a voluminous quantity of CSF directly streams into the blocked SAS/BC leading to a recurrent ↑ICP which is liable to be viewed as a failure [23–27].
3. Although a sequence of LPs should always be performed in patients who remain symptomatic/↑ICP, before ETV is assumed to have failed [23–25], in our delicate patients' population we could apply LP in selected cases. Instead, we took the advantage of our curved reservoir skin incision with subgaleal pocket technique to accommodate released CSF during the early adaptation period [2]. This idea allows the CSF to egress via a reverse brilliant manner (to be absorbed in the subgaleal pocket) to escape questionable acute obstruction. It allows the natural intermittent controlled CSF release/absorption according to the infant's own needs [2].
4. CSF release recovers the compliance and buffering capacity of the SAS/BC [6–12].

Limitations and ideas to overcome them

The retrospective nature of this single-institution study along with the relatively small number of the included infants might be considered a limitation. Besides, a surgeon's learning curve can affect the degree of maneuverability in such challenging cases and the overall outcome. To overcome these limitations, it is reasonable to have a multicenter engaged in a prospective trial to further validate and/or modify this unique traffic light concept for both adult and pediatric populations.

Conclusions

Traffic light ETV-DS and ETV-FT are easily interpretable/memorable alarming signs for robust decision-making. They can warn neurosurgeons to distinguish challenging patients that require ultra-precautions to navigate safely through landmines for worthy outcomes. It can be validated in delicate patient populations including neonates, babies, and young infants >1 year.

Abbreviations

↑ICP	Increased intracranial pressure
AnLS	Aneurysm-like structure
Aq.Slv	Aqueduct of Sylvius
BA	Basilar artery
CPC	Choroid plexus coagulation
CSF	Cerebrospinal fluid
DEBA	Dolicoectatic BA
DS	Dorsum sellae
ETV	Endoscopic third ventriculostomy
ETV-DS	ETV difficulty scale
ETV-FT	ETV failure threshold
FAEC	Fogarty arterial embolectomy catheters
FM	Foramen of Monro
HC	Head circumference
III-VT	Third ventricle
LM	Liliequist membrane
LP	Lumbar puncture
MB	Mammillary bodies
PC-MRI	Cine phase contrast-magnetic resonance image
SAS/BC	Subarachnoid space and/or basal cisterns
SG	Subgaleal
SSAJ	Scissors with single action jaw
TC	Tuber cinerium

Acknowledgements

Not applicable

Author contributions

The conception, design, administrative, technical, and material support were done by the corresponding author (AN).

Funding
Not applicable

Availability of data and materials
All data used are available from the corresponding author on request.

Declarations

Ethics approval and consent to participate
In compliance with ethical standards, University's research ethics committee approval and consents, from all patients' parents/guardians who participated in this study, were obtained.

Consent for publication
Was obtained from all patients' parents/guardians who participated in this study.

Competing interests
The authors declare that they have no competing interests.

Received: 2 March 2023 Accepted: 4 April 2023
Published online: 30 October 2023

References

1. Kulkarni AV, Drake JM, Mallucci CL, Sgouros S, Roth J, Constantini S; Canadian Pediatric Neurosurgery Study Group. Endoscopic third ventriculostomy in the treatment of childhood hydrocephalus. J Pediatr. 2009; 155:254–259
2. Nagm A. Endoscopic Third Ventriculostomy: The Art of Driving. AIMJ. 2023; (in press).
3. Nagm A, Hemdan A, Salem A. Neuroendoscopic unrestricted Access to and visualization of the important anatomical structures at the third ventricle: Surgical implications and image record. AIMJ. 2022;3(10):168–73.
4. Nagm A, Ogiwara T, Goto T, Chiba A, Hongo K. Neuroendoscopy via an extremely narrow foramen of monro: a case report. NMC Case Rep J. 2016;4:37–42.
5. Zohdi A, Elkheshin S. Endoscopic anatomy of the velum interpositum: a sequential descriptive anatomical study. Asian J Neurosurg. 2012;7:12–6.
6. Hassanien Omar A, Abo-Dewan Khalid A, Mahrous Omar M, El Kheshin Shiref E. Evaluation of the patency of endoscopic third ventriculostomy using phase contrast MRI-CSF flowmetry as diagnostic approach. Egypt J Radiol Nucl Med. 2018;49:701–10.
7. Deopujari CE, Karmarkar VS, Shaikh ST. Endoscopic third ventriculostomy: success and failure. J Korean Neurosurg Soc. 2017;60:306–14.
8. Alves T, Ibrahim ES, Martin BA, Malyarenko D, Maher C, Muraszko KM, Garton HJ, Srinivasan A, Bapuraj JR. Principles, techniques, and clinical applications of phasecontrast magnetic resonance cerebrospinal fluid imaging. Neurographics. 2017;7:199–210.
9. Stovell MG, Zakaria R, Ellenbogen JR, Gallagher MJ, Jenkinson MD, Hayhurst C, Mallucci CL. Long-term follow-up of endoscopic third ventriculostomy performed in the pediatric population. J Neurosurg: Pediat. 2016;17:734–8.
10. Öztürk M, Sığırcı A, Ünlü S. Evaluation of aqueductal cerebrospinal fluid flow dynamics with phase-contrast cine magnetic resonance imaging in normal pediatric cases. Clin Imaging. 2016;40:1286–90.
11. Anik I, Etus V, Anik Y, Ceylan S. Role of interpeduncular and prepontine cistern cerebrospinal fluid flow measurements in prediction of endoscopic third ventriculostomy success in pediatric triventricular hydrocephalus. Pediat Neurosurg. 2010;46:344–50.
12. Kandasamy J, Yousaf J, Mallucci C. Third ventriculostomy in normal pressure hydrocephalus. World Neurosurg. 2013;79:S22-31.
13. Bargalló N, Olondo L, Garcia AI, Capurro S, Caral L, Rumia J. Functional analysis of third ventriculostomy patency by quantification of CSF stroke volume by using cine phase-contrast MR imaging. Am J Neuroradiol. 2015;26:2514–21.
14. Lev S, Bhadelia RA, Estin D, Heilman CB, Wolpert SM. Functional analysis of third ventriculostomy patency with phase-contrast MRI velocity measurements. Neuroradiology. 1997;39:175–9.
15. Nitz WR, Bradley WG Jr, Watanabe AS, Lee RR, Burgoyne B, O'Sullivan RM, Herbst MD. Flow dynamics of cerebrospinal fluid: assessment with phase-contrast velocity MR imaging performed with retrospective cardiac gating. Radiology. 2002;183:395–405.
16. Woodworth G, McGirt MJ, Thomas G, Williams MA, Rigamonti D. Prior CSF shunting increases the risk of endoscopic third ventriculostomy failure in the treatment of obstructive hydrocephalus in adults. Neurol Res. 2007;2007(29):27–31.
17. Jaeger M, Khoo AK, Conforti DA, Cuganesan R. Relationship between intracranial pressure and phase contrast cine MRI derived measures of intracranial pulsations in idiopathic normal pressure hydrocephalus. J Clin Neurosci. 2016;30:169–72.
18. Oner Z, Sagir Kahraman A, Kose E, Oner S, Kavakli A, Cay M, Ozbag D. Quantitative evaluation of normal aqueductal cerebrospinal fluid flow using phase contrast cine mri according to age and sex. Anatom Record. 2017;300:549–55.
19. Wagner W, Koch D. Mechanisms of failure after endoscopic third ventriculostomy in young infants. J Neurosurg. 2005;103(1 Suppl):43–9.
20. Hu Z, Kang Z, Zhu G, Tu J, Huang H, Guan F, Dai B, Mao B. Experience with lumbar puncture following endoscopic third ventriculostomy for obstructive hydrocephalus. J Neurol Surg A Cent Eur Neurosurg. 2017;78:132–6.
21. Bellotti A, Rapanà A, Iaccarino C, Schonauer M. Intracranial pressure monitoring after endoscopic third ventriculostomy: an effective method to manage the "adaptation period." Clin Neurol Neurosurg. 2001;103:223–7.
22. Nishiyama K, Mori H, Tanaka R. Changes in cerebrospinal fluid hydrodynamics following endoscopic third ventriculostomy for shunt-dependent noncommunicating hydrocephalus. J Neurosurg. 2003;98:1027–31.
23. Tubbs RS, Vahedi P, Loukas M, Cohen-Gadol AA. Harvey Cushing's experience with treating childhood hydrocephalus: in his own words. Childs Nerv Syst. 2011;27:995–9.
24. Beni-Adani L, Biani N, Ben-Sirah L, Constantini S. The occurrence of obstructive vs absorptive hydrocephalus in newborns and infants: relevance to treatment choices. Childs Nerv Syst. 2006;22:1543–63.
25. Cinalli G, Spennato P, Ruggiero C, Aliberti F, Zerah M, Trischitta V, Cianciulli E, Maggi G. Intracranial pressure monitoring and lumbar puncture after endoscopic third ventriculostomy in children. Neurosurgery. 2006;58:126–36 (**discussion 126–136**).
26. Rapanà A, Bellotti A, Iaccarino C, Pascale M, Schönauer M. Intracranial pressure patterns after endoscopic third ventriculostomy. Preliminary experience. Acta Neurochir (Wien). 2004;146:1309–15 (**discussion 1315**).
27. Yadav YR, Mukerji G, Parihar V, Sinha M, Pandey S. Complex hydrocephalus (combination of communicating and obstructive type): an important cause of failed endoscopic third ventriculostomy. BMC Res Notes. 2009;2:137.
28. Lenfeldt N, Koskinen LO, Bergenheim AT, Malm J, Eklund A. CSF pressure assessed by lumbar puncture agrees with intracranial pressure. Neurology. 2007;68:155–8.
29. Obaid S, Weil AG, Rahme R, Bojanowski MW. Endoscopic third ventriculostomy for obstructive hydrocephalus due to intraventricular hemorrhage. J Neurol Surg A Cent Eur Neurosurg. 2015;76:99–111.
30. Cinalli G, Sainte-Rose C, Chumas P, Zerah M, Brunelle F, Lot G, Pierre-Kahn A, Renier D. Failure of third ventriculostomy in the treatment of aqueductal stenosis in children. J Neurosurg. 1999;90:448–54.
31. Javadpour M, Mallucci C, Brodbelt A, Golash A. The impact of endoscopic third ventriculostomy on the management of newly diagnosed hydrocephalus in infants. Pediatr Neurosurg. 2001;35:131–5.
32. Milhorat TH, Hammock MK, Di Chiro G. The subarachnoid space in congenital obstructive hydrocephalus. 1. Cisternographic findings. J Neurosurg. 1971;35:1–6.
33. Kulkarni AV, Riva-Cambrin J, Rozzelle CJ, Naftel RP, Alvey JS, Reeder RW, Holubkov R, Browd SR, Cochrane DD, Limbrick DD, Simon TD, Tamber M, Wellons JC, Whitehead WE, Kestle JRW. Endoscopic third ventriculostomy and choroid plexus cauterization in infant hydrocephalus: a prospective study by the Hydrocephalus Clinical Research Network. J Neurosurg Pediatr. 2018;21:214–23.
34. Fallah A, Weil AG, Juraschka K, Ibrahim GM, Wang AC, Crevier L, Tseng CH, Kulkarni AV, Ragheb J, Bhatia S. The importance of extent of choroid

plexus cauterization in addition to endoscopic third ventriculostomy for infantile hydrocephalus: a retrospective North American observational study using propensity score-adjusted analysis. J Neurosurg Pediatr. 2017;20:503–10.
35. Zandian A, Haffner M, Johnson J, Rozzelle CJ, Tubbs RS, Loukas M. Endoscopic third ventriculostomy with/without choroid plexus cauterization for hydrocephalus due to hemorrhage, infection, Dandy-Walker malformation, and neural tube defect: a meta-analysis. Childs Nerv Syst. 2014;30:571–8.
36. Dewan MC, Naftel RP. The global rise of endoscopic third ventriculostomy with choroid plexus cauterization in pediatric hydrocephalus. Pediatr Neurosurg. 2017;52:401–8.
37. Stone SS, Warf BC. Combined endoscopic third ventriculostomy and choroid plexus cauterization as primary treatment for infant hydrocephalus: a prospective North American series. J Neurosurg Pediatr. 2014;14:439–46.
38. Roth J, Constantini S. Combined rigid and flexible endoscopy for tumors in the posterior third ventricle. J Neurosurg. 2015;122:1341–6.
39. Tjemme B, Andre GJ. Long term complications and definition of failure of neuroendoscopic procedures. Childs Nerv Syst. 2004;20:868–77.
40. Mortazavi MM, Rizq F, Harmon O, Adeeb N, Gorjian M, Hose N, Modammadirad E, Taghavi P, Rocque BG, Tubbs RS. Anatomical variations and neurosurgical significance of Liliequist's membrane. Childs Nerv Syst. 2015;31:15–28.
41. Anık I, Ceylan S, Koc K, Anık Y, Etus V, Genc H. Membranous structures affecting the success of endoscopic third ventriculostomy in adult aqueductus sylvii stenosis. Minim Invasive Neurosurg. 2011;54:68–74.
42. Anik I, Ceylan S, Koc K, Tugasaygi M, Sirin G, Gazioglu N, Sam B. Microsurgical and endoscopic anatomy of Liliequist's membrane and the prepontine membranes: cadaveric study and clinical implications. Acta Neurochir (Wien). 2011;153:1701–11.
43. Sughrue ME, Chiou J, Burks JD, Bonney PA, Teo C. Anatomic variations of the floor of the third ventricle: an endoscopic study. World Neurosurg. 2016;90:211–27.
44. Karvonen M, Saari A, Lamidi ML, Selander T, Löppönen T, Lönnqvist T, Dunkel L, Sankilampi U. Screening of hydrocephalus in infants using either WHO or population-based head circumference reference charts. Acta Paediatr. 2021;110:881–8.
45. Oertel J, Linsler S, Csokonay A, Schroeder HWS, Senger S. Management of severe intraoperative hemorrhage during intraventricular neuroendoscopic procedures: the dry field technique. J Neurosurg. 2018;131:931–93.

Publisher's Note